B and N ion implantation into carbon nanotubes: Insight from atomistic simulations

J. Kotakoski,[1] A. V. Krasheninnikov,[1,2] Yuchen Ma,[2] A. S. Foster,[2] K. Nordlund,[1] and R. M. Nieminen[2]
[1]*Accelerator Laboratory, P.O. Box 43, FIN-00014 University of Helsinki, Finland*
[2]*Laboratory of Physics, Helsinki University of Technology, P.O. Box 1100, 02015, Finland*
(Received 25 January 2005; published 23 May 2005)

By employing atomistic computer simulations with empirical potential and density functional force models, we study B/N ion implantation onto carbon nanotubes. We simulate irradiation of single-walled nanotubes with B and N ions and show that up to 40% of the impinging ions can occupy directly the sp^2 positions in the nanotube atomic network. We further estimate the optimum ion energies for direct substitution. *Ab initio* simulations are used to get more insight into the structure of the typical atomic configurations which appear under the impacts of the ions. As annealing should further increase the number of sp^2 impurities due to dopant atom migration and annihilation with vacancies, we also study migration of impurity atoms over the tube surface. Our results indicate that irradiation-mediated doping of nanotubes is a promising way to control the nanotube electronic and even mechanical properties due to impurity-stimulated crosslinking of nanotubes.

DOI: 10.1103/PhysRevB.71.205408 PACS number(s): 81.07.De, 61.80.Jh, 85.40.Ry

I. INTRODUCTION

Since the discovery of carbon nanotubes in 1991,[1] the outstanding mechanical and electronic properties of these tubular molecules have stimulated much research on nanotube applications. One of the major goals has been to use nanotubes in electronics as, in addition to their inherent nanometer sizes, they can be either semiconductors or metals.[2] The electronic properties of the nanotube are determined by the tube chirality.[2] Unfortunately, as-grown nanotubes present a mixture of tubes with different chiralities, and despite a substantial effort,[3] at the moment there is no way to reliably separate nanotubes according to their electronic structure.

Similar to conventional semiconductor technology, the electronic properties of nanotubes can be tailored by introducing impurities. To this end, it has been suggested to dope carbon nanotubes with B and/or N atoms.[4–12] This is a natural choice of the dopant, as B/N have roughly the same atomic radius as C, while they possess one electron less/more than C, respectively. N doping has received particular attention, as N impurities can also give rise to nanotube functionalization,[5] and transformations of the atomic network to bamboo-like structures,[6,7] which can enhance field emission.[10]

Several methods based on arc-discharge techniques[6,13] and substitutional reactions[8] have been developed for doping. Unfortunately, instead of occupying the substitutional sp^2 position in the graphitic network, a substantial part of the dopant is chemisorbed[14] on the nanotube surface, forms nitrogen molecules intercalated between graphite layers,[11] or binds to irregular carbon structures in sp^3 sites.[6] Besides this, substitutional reactions with N atoms seem to be almost impossible for nanotubes with diameters less than 8 nm.[8] Problems with incorporating B atoms into the carbon lattice of nanotubes have also been reported.[13] All of these issues further limit the applicability of these techniques.

In this paper, we offer an alternative way to introduce B/N impurities into nanotubes. We suggest using ion irradiation as a tool to dope nanotubes with B and N. Ion beams have been used to implant N^+ ions into graphite[15] and fullerene solids,[16] but, to the best of our knowledge, this technique has not yet been used for carbon nanotubes. We stress that nanotubes are nano-objects with a unique atomic structure, and thus it is not clear *a priori* if it is possible to introduce substitutional impurities by irradiating them. Further, the probability of direct substitution and the optimum ion energy for implantation are also unknown.

Making use of molecular dynamics with analytical potentials we simulate irradiation of single-walled nanotubes (SWNTs) with B and N atoms and show that up to 40% of the impinging ions can directly occupy the sp^2 positions in the nanotube atomic network. We also estimate the optimum ion energies for the direct substitution. We further use density functional theory (DFT) to obtain more insight into the geometry and electronic structure of the typical atomic configurations that appear under impacts of the ions. As annealing should further increase the number of sp^2 impurities due to dopant atom migration and occupying the empty positions at vacancies, we also study migration of impurity atoms over the tube surface. Our simulations indicate that B and N adatoms on the nanotube surface are highly mobile at room temperature, and thus a further increase in the number of sp^2 dopant atoms is possible after annealing due to the vacancy-mediated mechanism[8] of substitution.

II. SIMULATION METHODS

To simulate impacts of B/N impurity atoms into SWNTs, we employed classical molecular dynamics (MD) with empirical (analytical) potentials. The simulation method is described at length in our previous publications,[17,18] and therefore we present here only the details essential for this study. The interactions between atoms of different types (C—B/N) were described by a Tersoff-like potential by Matsunaga *et al.*[19] To realistically model energetic collisions, we smoothly joined the potentials with the Ziegler-Biersack-Littmark repulsive potentials[20] at short interatomic separations.[21] We did not account for the electronic stopping as the ion energies

were low and the nuclear slowing down governed the collisional phase.

To get more insight into the structures and energetics of the typical atomic configurations which appear under irradiation, we also ran DFT calculations. We used the plane wave basis VASP code,[22,23] implementing the generalized gradient approximation of Perdew *et al.*[24] We used projected augmented wave potentials[25,26] to describe the core ($1s^2$) electrons. A kinetic energy cutoff of 400 eV was found to converge the total energy of our systems to within 1 meV. Brillouin zone sampling is performed using the *k*-points generation scheme of Monkhorst-Pack[27] (Γ-point included).

We stress that dynamical simulations of B/N ion impacts onto nanotubes can nowadays be carried out by employing empirical potentials only, as DFT dynamical calculations are computationally too expensive, since many runs with different impact parameters are required to obtain comprehensive statistics. Note that the analytical potential we used was developed for cubic boron-carbon-nitride systems and its parameterization did not include any graphitic systems with sp^2-hybridization of atoms. Thus, one could not expect a perfect agreement between the DFT and empirical potential data. However, as we show below, all the irradiation-induced atomic configurations calculated by the empirical method proved to be stable within the DFT approach, and the geometry and energetics of the typical impurity atom-nanotube atomic configurations calculated by the empirical potential and DFT methods are in qualitative agreement.

As an additional test for the dynamical simulations of ion impacts, we also ran simulations with the Brenner II potential[28] (with parameters for carbon), assuming that B and N atoms are chemically equivalent to C, but with the correct atomic mass. This made it possible to assess how sensitive to the potential parameters the results of calculations were. We obtained very close data on the defect distribution and appearance probabilities,[29] which indicated that the results depended only weakly on chemical interactions; rather they were governed by the collisional phase.

III. RESULTS AND DISCUSSION

A. Dynamical simulations of N/B ion impacts onto SWNTs

We started with dynamical simulations of SWNT bombardment with B and N ions.[30] We considered individual armchair (10,10) SWNTs with a diameter of 1.4 nm. We simulated impacts of the ions with different energies onto a 100 Å long SWNT. The ion impact points were randomly chosen. The ion beam direction was assumed to be perpendicular to the SWNT axis. To obtain representative statistics, for each ion energy we ran 200 independent simulations and averaged the results. Periodic boundary conditions were employed, and the Berendsen temperature control technique[31] was used at the tube boundaries to account for the energy dissipation at the borders. The simulation temperature was chosen to be 0 K (the system temperature before the ion impact). When the collisional phase was over, the system was quenched to zero temperature over 30 ps, which is the typical time of epithermal energy dissipation in carbon systems.[32]

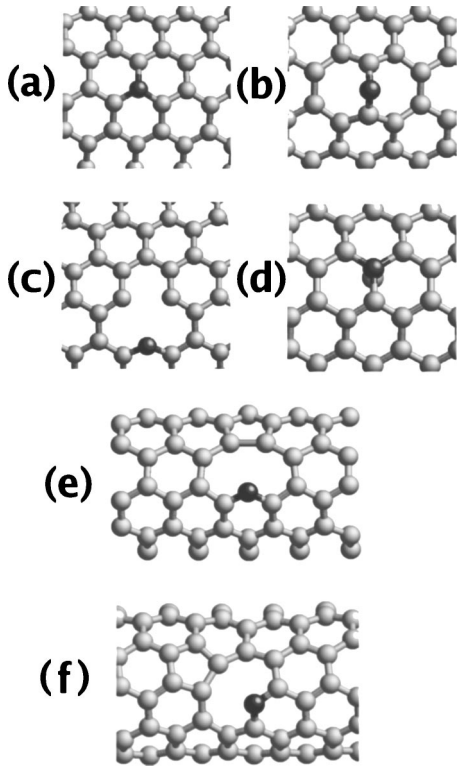

FIG. 1. Most abundant atomic configurations after B/N ion impacts onto single-walled carbon nanotubes. (a) perfect sp^2 impurity, (b) bridge, (c) rocket, and (d) sp^2+C configurations in a (10,10) SWNT as calculated with the analytical model. The dark spheres represent the dopant atom, the light ones carbon atoms. (e) and (f) The rocket configurations in a (5,5) SWNT as calculated with the DFT model. Note partial mending of the defects by dangling bond saturation.

As finite temperatures can be important for the defect evolution, we also studied the annealing of defects. In these simulations, after the completion of the collisional phase we increased the temperature up to 1500 K and simulated the system behavior for 0.1 ns. This computational technique made it possible to account, at least partially, for defect annealing at low/room temperatures but on a macroscopic time scale, and thus get rid of spurious metastable configurations.[17]

To differentiate between direct and annealing-mediated substitution, we analyzed defect configurations before and after the annealing. We found that there are four different implant atom-SWNT configurations which dominate for both B and N. These configurations are shown in Fig. 1. The most important configuration is the perfect sp^2 position of the dopant in the nanotube atomic network [see Fig. 1(a)]. Another widespread configuration, especially at low energies of the ions, is the B/N adatom on the tube surface [Fig. 1(b)].

In addition to these two configurations, the most prolific atomic configurations proved to be as follows: in the "rocket" defect type, the impact of the dopant atom has displaced a C away from the SWNT network and has replaced another C (two carbon atoms are missing cf. sp^2 defect) [Fig. 1(c)]; in the sp^2+C defect type [Fig. 1(d)], the dopant atom has replaced a carbon atom that remains bonded to the dop-

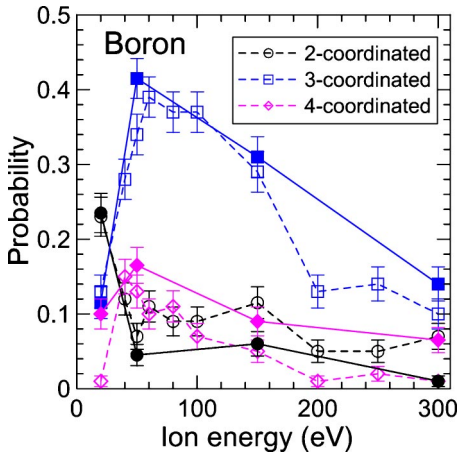

FIG. 2. Probabilities for coordination numbers for B as functions of the initial ion energy. The open/full symbols stand for the results before/after the annealing.

ant. This configuration was particularly common for B. These defect types make up 70%–80% of all final configurations for bonded B before and 70%–90% after the annealing. For bonded N these probabilities are 45%–85% and 50%–80%, respectively.

An alternative way to analyze the overall effect of ion impacts onto nanotubes is to count the number of nearest neighbors (the coordination number) of the dopant atoms. We calculated the coordination number for every dopant atom after every run. The number of dopant atoms with different coordinations per one impinging ion (coordination number probabilities) are shown in Figs. 2 and 3 for B and N, respectively, as functions of ion energy. It is evident that the probabilities for three-coordinated dopant atoms have maxima near 50 eV. For boron, the probability can be up to 40%, and almost 50% for nitrogen.

Note that at low ion energies the ion can be bounced back by the tube (or just scattered), so that the ion remains zero coordinated. Thus, the sum over all probabilities shown in Figs. 2 and 3, and Table I is less than unity. The fraction of

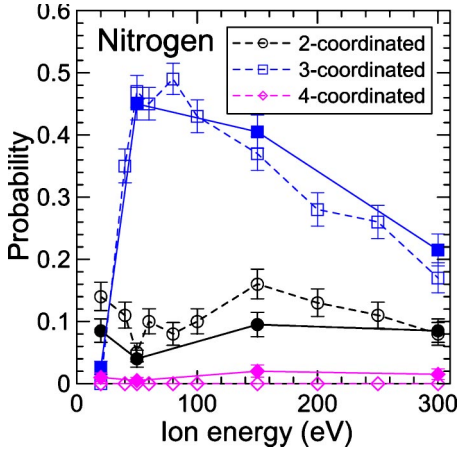

FIG. 3. Probabilities for coordination numbers for N as functions of the initial ion energy. The open/full symbols stand for the results before/after the annealing.

TABLE I. Defect types and their relative abundance (the probability to appear) before (the first row) and after annealing (the second row). V_C is the number of missing C atoms, i.e., C vacancies. Note that because some dopant atoms are scattered away from or transmitted through the tube, the sum of all cases is less than unity. The total abundance of defects does in some cases increase after annealing when atoms which are zerofold bonded before annealing bond with the tube network during annealing. The estimated standard deviation is about 0.05 in the values presented in the table.

		Boron			Nitrogen		
Type	V_C	50 eV	150 eV	300 eV	50 eV	150 eV	300 eV
sp^2	1	0.30	0.23	0.09	0.40	0.16	0.17
		0.28	0.27	0.12	0.40	0.39	0.11
Bridge	0	0.04	0.01	0.01	0.03	0.05	0.01
		0.05	0.00	0.00	0.00	0.00	0.02
Rocket	2	0.00	0.03	0.00	0.00	0.03	0.01
		0.00	0.00	0.00	0.00	0.03	0.03
sp^2	0	0.15	0.02	0.00	0.00	0.00	0.00
+C		0.15	0.05	0.00	0.00	0.00	0.00
Other		0.14	0.23	0.13	0.19	0.37	0.12
Bonded		0.25	0.27	0.20	0.19	0.20	0.23

ions that remains in the tube decreases with energies above 50 eV.

If we only consider those dopants that stay in the tube, the values in Table I show that the probability for dopant atoms in the tube to achieve the substitutional sp^2 configuration is about 50% for B and 65% for N at 50 eV before annealing. At 300 eV the corresponding probabilities are 40% for B and 55% for N. From these numbers one notices that the probability of achieving the sp^2 configuration (for dopants staying in the tube) decreases only relatively weakly with energy. However, note that the relative amount of complex defect types increases with energy. Hence, the lowest energies are still the best to achieve high fractions of substitutional sp^2 defects.

The probability maximum at ~50 eV can be understood in terms of kinetic energy transfer. In our force model, a C atom must have a kinetic energy of about 25 eV to leave its position in the atomic network. Within the binary collision approximation, this corresponds to energies of ions of about 30 eV (for a head-on collision). However, the impact parameter is randomly distributed, so that on average the ion should have a higher energy. Besides this, an additional energy is required due to multi-atom interactions governed by the cutoff range—the ion kinetic energy is transferred to both the recoil and its environment. When the ion energy further increases, the ions just go through the nanotube. Note that the number of defects in the nanotube atomic network also decreases at higher energies due to lower momentum transfer.[18]

As dopant atoms can have the same coordination in different atomic configurations, we carried out a more detailed analysis of the final structures and the dopant bonding. The relative probabilities of the defects to appear are listed in

Table I for different defect types. The maximum probabilities for dopant atoms to end up in the sp^2 configuration are ~30% for B and ~40% for N. Thus, nearly all three-coordinated impurity atoms are in the sp^2 configuration.

We obtained qualitatively similar results for (5,5) SWNTs. We did not systematically study how the optimum energy depends on the SWNT diameter, but our simulations unambiguously show that substitution is possible for nanotubes with arbitrary diameters. Thus, if indeed the substitution reaction mechanism does not work for nanotubes with diameters less than 8 nm,[8] the irradiation-mediated method should be able to overcome the limitations of the chemical methods.

B. Density functional theory calculations of dopant atom-nanotube configurations

In order to get more insight into the structures and energetics of the typical atomic configurations which appear after irradiation, we ran DFT calculations as described above. Throughout this section, when listing the numbers, we refer to the results of DFT simulations unless stated otherwise.

We chose a graphite sheet and a (5,5) SWNT as the two limiting cases. The curvature of the (10, 10) tubes used in irradiation simulations is between that of the (5, 5) tube and the graphite. The (10, 10) and (5, 5) tubes have the same chirality, so the properties of the (10, 10) tubes used in the dynamical simulations could be interpolated from those of the graphite and the (5, 5) tube.

We first calculated the energies of B/N atoms in the sp^2 substitution configurations [see Fig. 1(a)]. We found that it costs 1.86 and 1.76 eV to substitute a carbon atom with N in a graphite sheet and (5, 5) tube, respectively. A very similar value of 1.7 eV was recently obtained for a (5, 5) tube.[12] The decrease in the formation energy from graphite to the (5, 5) tube is consistent with the proposal that N atom prefers a nonplanar surrounding in the graphitic materials,[33,34] although the actual buckling occurs at concentrations of N atoms exceeding 20%.[33] Calculations for (7,0) and (9,0) SWNTs gave 1.24 and 1.61 eV, respectively, which further validates this assumption. For B dopant atoms, the cost of substitution is 3.64 eV for graphite and 3.08 eV for a (5,5) SWNTs.

As for adatoms on graphene and the outer surface of the tubes [Fig. 1(b)], both N and B adatoms occupy the *bridge* position on top of C—C bonds, similar to C adatoms.[35,36] Note that in nanotubes there are two different kinds of bonds (oriented parallel/perpendicular to the tube axis.[36] In what follows, we refer to the "perpendicular" configurations, which are always lower in energy.

When the N atom is in the bridge configuration on the graphite plane, the distance between the N atom and the nearest neighbor is 1.45 Å. The adsorption energy is 3.94 eV. The two C atoms bonded to the N atom become sp^3-hybridized and the distance between them is 1.58 Å. However, the interaction between the B adatom and the graphite is much weaker. The adsorption energy is 1.27 eV. The distance between the B atom and the nearest carbon atom is 1.83 Å and the distortion of the graphite sheet is much smaller. The C—C bond between the two carbon atoms nearest to the B atom increases to 1.47 Å. For the N/B adatoms adsorbed on the outer surface of the (5,5) SWNT [Fig. 1(b)], the N/B atom breaks the C—C bond between the two carbon atoms bonded to the N/B atoms, occupying out-of-plane positions. The length of the N—C/B—C bonds are 1.40 Å/1.49 Å, and the adsorption energies are 5.81 eV/2.76 eV.

DFT calculations for the rocket configuration in a (5,5) SWNT showed that the saturation of dangling bonds gives rise to a drop in energy and that the configuration showed in Fig. 1(f) has the lowest energy. The analytical potential gave the same results for (5,5) tubes, but for tubes with larger diameters the reconstruction did not occur. For the rocket configuration in graphite, the distance between the two two-coordinated carbon atoms is 1.88 Å. Electron density contours show that there is weak interaction between them.

It is worth mentioning that all atomic configurations that appeared after irradiation proved to be stable within both the DFT and empirical potential approaches. The analytical potential results gave different values of the adsorption/substitution energies, but nevertheless, correctly reproduced the effect of curvature on the energetics.

C. Diffusion of dopant atoms and their recombination with vacancies

One can expect that annealing should further increase the number of sp^2 impurities due to dopant atom migration and annihilation with vacancies created by energetic recoils. Indeed, even when the ion energy is higher than optimal for direct substitution, every impact creates many vacancies. Consequently, if the dopant atoms are mobile in the sample, they will likely find a vacancy and recombine with it. Knowing the dopant atom migration energies is also indispensable for understanding electron irradiation-induced transformations in nanotubes and other B—C—N systems.[37]

In our dynamical calculations we partly took into account the annealing of defects on the macroscopic time scale by elevating the temperature and running simulations for a short time. However, Tersoff-like potentials are known to overestimate the migration barrier due to the presence of a finite cutoff for atom interactions.[36] To obtain more reliable data, we calculated the barrier for N/B adatoms on a graphene sheet by the DFT method. We could not systematically calculate the barriers for tubes with different diameters due to computational limitations, but, similar to the case of carbon adatoms on the outer surface of nanotubes, the finite curvature should be important only for nanotubes with diameters less than 1 nm.[36]

We used the nudged elastic band method[38,39] implemented into VASP to determine minimum barrier energy diffusion paths between known initial and final atomic configurations. The nudged elastic band method starts from a chain of configurations interpolating between the initial and the final geometries. The atomic positions in the different configurations are then iteratively optimized using only the ionic-force components perpendicular to the hypertangent.

The energy barrier for the N/B adatoms to migrate to the adjacent equilibrium bridge-like position were found to be

1.1/0.1 eV, with the migration path being a nearly straight line connecting the adjacent equilibrium positions, similar to that of the carbon adatom on the graphite surface.[35] Note also that for adatoms inside the tube, the migration barrier should be even smaller due to the negative curvature. Thus, the dopant atoms, especially boron, are mobile at room temperatures, which should facilitate the annealing.

IV. DISCUSSION AND CONCLUSIONS

Making use of molecular dynamics with analytical potentials, we simulated irradiation of single-walled nanotubes with low-energy B and N ions. We showed that up to 40% of the impinging ions can occupy directly the sp^2 positions in the nanotube atomic network. Given that at optimum ion energies about 65% of the impinging ions get stuck in the tube, this value makes up two thirds of the stopped ions. This is a remarkably high number if one compares it, e.g., to the doping of conventional semiconductors like Si, where high-temperature annealing is usually needed to achieve a sizeable fraction of substitutional positions.[40]

We also estimated the optimum ion energies for the direct substitution, which are around 50 eV. We showed that, in addition to the perfect substitutional position, the dopant atom can form other stable/metastable configurations with the carbon atoms at the surface of the intact nanotube and a nanotube with irradiation-induced vacancies.

We further ran *ab initio* simulations to get more insight into the structure and energetics of the typical dopant atom/defect configurations that appear under the impacts of the ions. As annealing should further increase the number of sp^2 impurities due to dopant atom migration and annihilation with vacancies, we also studied migration of impurity atoms over the tube surface. We found that the migration barriers for nitrogen and boron adatoms are 1.1 and 0.1 eV, respectively. Thus both types of adatoms should be mobile at room temperature, and a further increase in the number of sp^2 dopant atoms is possible after sample annealing due to recombination of the dopant adatoms with vacancies.[8]

As dopant atoms change the local electronic structure of the nanotube,[5–10,12] our results indicate that irradiation-mediated doping of nanotubes is a promising way to control the nanotube electronic properties. In particular, by employing spatially localized ion irradiation, it is further possible to dope predetermined parts of the nanotube, and thus make a superstructure, which can lead to the development of new nanotube-based electronic devices. In such experiments, other carbon nanotubes can be used as masks[41] to protect the areas of the irradiated tube. Mechanical properties of the nanotube macroscopic samples can be altered as well due to impurity-stimulated crosslinking between graphitic shells[42] and individual nanotubes.[5]

In conclusion, our results show that low-energy ion implantation is a promising way to achieve a high fraction of substitutional B and N dopants in a carbon nanotube atomic network.

ACKNOWLEDGMENTS

The research was supported by the Academy of Finland under Project Nos. 48751, 50578, and 202737, the Academy of Finland Center of Excellence Program (2000–2005), and partially by the ELENA project within the Academy of Finland TULE program. Grants of computer time from the Center for Scientific Computing in Espoo, Finland are gratefully acknowledged.

[1] S. Iijima, Nature (London) **354**, 56 (1991).
[2] *Carbon Nanotubes, Synthesis, Structure, Properties and Applications*, edited by M. S. Dresselhaus, G. Dresselhaus, and P. Avouris (Springer, Berlin, 2001).
[3] R. C. Haddon, J. Sippel, A. G. Rinzler, and F. Papadimitrakopoulos, MRS Bull. **29**, 252 (2004).
[4] M. Terrones *et al.*, Appl. Phys. A: Mater. Sci. Process. **65**, 355 (2002).
[5] A. H. Nevidomskyy, G. Csányi, and M. C. Payne, Phys. Rev. Lett. **91**, 105502 (2003).
[6] R. Droppa, Jr., C. T. M. Ribeiro, A. R. Zanatta, M. C. dos Santos, and F. Alvarez, Phys. Rev. B **69**, 045405 (2004).
[7] J. W. Jang, C. E. Lee, S. C. Lyu, T. J. Lee, and C. J. Lee, Appl. Phys. Lett. **84**, 2877 (2004).
[8] D. Srivastava, M. Menon, C. Daraio, S. Jin, B. Sadanadan, and A. M. Rao, Phys. Rev. B **69**, 153414 (2004).
[9] L. H. Chan, K. H. Hong, D. Q. Xiao, T. C. Lin, S. H. Lai, W. J. Hsieh, and H. C. Shih, Phys. Rev. B **70**, 125408 (2004).
[10] R. C. Che, L.-M. Peng, and M. S. Wang, Appl. Phys. Lett. **85**, 4753 (2004).
[11] H. C. Choi, S. Y. Bae, J. Park, K. Seo, C. Kim, B. Kim, H. J. Song, and H.-J. Shin, Appl. Phys. Lett. **85**, 5742 (2004).
[12] H. S. Kang and S. Jeong, Phys. Rev. B **70**, 233411 (2004).
[13] M. Glerup, J. Steinmetz, D. Samaille, O. Stéphan, S. Enouz, A. Loiseau, S. Roth, and P. Bernier, Chem. Phys. Lett. **387**, 193 (2004).
[14] Q. Zhao, M. B. Nardelli, and J. Bernholc, Phys. Rev. B **65**, 144105 (2002).
[15] I. Shimoyama, G. Wu, T. Sekiguchi, and Y. Baba, Phys. Rev. B **62**, R6053 (2000).
[16] M. Mehring, W. Scherer, and A. Weidinger, Phys. Rev. Lett. **93**, 206603 (2004).
[17] A. V. Krasheninnikov, K. Nordlund, M. Sirviö, E. Salonen, and J. Keinonen, Phys. Rev. B **63**, 245405 (2001).
[18] A. V. Krasheninnikov, K. Nordlund, and J. Keinonen, Phys. Rev. B **65**, 165423 (2002).
[19] K. Matsunaga, C. Fisher, and H. Matsubara, Jpn. J. Appl. Phys. **39**, L48 (2000).
[20] J. F. Ziegler, J. P. Biersack, and U. Littmark, *The Stopping and Range of Ions in Matter* (Pergamon, New York, 1985).
[21] K. Nordlund, J. Keinonen, and T. Mattila, Phys. Rev. Lett. **77**, 699 (1996).
[22] G. Kresse and J. Furthmüller, Comput. Mater. Sci. **6**, 15 (1996).
[23] G. Kresse and J. Furthmüller, Phys. Rev. B **54**, 11 169 (1996).
[24] J. P. Perdew, J. A. Chevary, S. H. Vosko, K. A. Jackson, M. R. Pederson, D. J. Singh, and C. Fiolhais, Phys. Rev. B **46**, 6671

(1992).
[25] G. Kresse and J. Joubert, Phys. Rev. B **59**, 1758 (1999).
[26] P. E. Blöchl, Phys. Rev. B **50**, 17 953 (1994).
[27] H. J. Monkhorst and J. D. Pack, Phys. Rev. B **13**, 5188 (1976).
[28] D. W. Brenner, Phys. Rev. B **42**, 9458 (1990).
[29] J. Kotakoski, J. Pomoell, A. V. Krasheninnikov, and K. Nordlund, Nucl. Instrum. Methods Phys. Res. B **228**, 31 (2005).
[30] The classical MD simulations cannot account for the charge state of atoms. Here we use the term ion to denote the incoming particle regardless of its charge state. We stress, however, that neutralization of the incoming ion occurs at the subfemtosecond time scale. Thus, at the low ion energies studied in this work, one can assume that the ion is neutral when it interacts with the target.
[31] H. J. C. Berendsen, J. P. M. Postma, W. F. van Gunsteren, A. DiNola, and J. R. Haak, J. Chem. Phys. **81**, 3684 (1984).
[32] F. Banhart, Rep. Prog. Phys. **62**, 1181 (1999).
[33] M. C. dos Santos and F. Alvarez, Phys. Rev. B **58**, 13 918 (1998).
[34] H. Sjöström, S. Stafström, M. Boman, and J. E. Sundgren, Phys. Rev. Lett. **75**, 1336 (1995).
[35] P. O. Lehtinen, A. S. Foster, A. Ayuela, A. Krasheninnikov, K. Nordlund, and R. M. Nieminen, Phys. Rev. Lett. **91**, 017202 (2003).
[36] A. V. Krasheninnikov, K. Nordlund, P. O. Lehtinen, A. S. Foster, A. Ayuela, and R. M. Nieminen, Phys. Rev. B **69**, 073402 (2004).
[37] D. Goldberg and Y. Bando, Recent Res. Devel. Applied Phys. **2**, 1 (1999).
[38] H. Jónsson, G. Mills, and G. K. Schenter, Surf. Sci. **324**, 305 (1995).
[39] H. Jonsson, G. Mills, and K. W. Jacobsen, *Nudged Elastic Band Method for Finding Minimum Energy Paths of Transitions*, in Classical and Quantum Dynamics in Condensed Phase Simulations (World Scientific, Singapore, 1998).
[40] E. Chason *et al.*, J. Appl. Phys. **81**, 6513 (1997).
[41] A. V. Krasheninnikov, K. Nordlund, and J. Keinonen, Appl. Phys. Lett. **81**, 1101 (2002).
[42] S. Stafström, Appl. Phys. Lett. **77**, 3941 (2000).